FINAL TECHNICAL REPORT

1. **DOE Award Number:** ER46979/SC0010693
   Institutions: Columbia University, University of Minnesota at Minneapolis
   Contact Info:

Prof. Xiaoyang Zhu
Department of Chemistry
Columbia
University
New York, NY 10027
Email: xyzhu@columbia.edu
Tel: 212-851-7768

Prof. C. Daniel Frisbie
Department of Chemical Engineering &
Materials Science
University of Minnesota
Minneapolis, MN 55455
Email: frisbie@umn.edu

2. **Project Title:** Spectroscopy of Charge Carriers and Traps in Field-Doped Single Crystal Organic Semiconductors
   Principal Investigator: Xiaoyang Zhu, C. Daniel Frisbie

3. **Date of the Report:** 03/31/2017
   Period Covered: 08/15/2013 – 12/31/2016

4. **Brief Description of Accomplishments**:

The proposed research aims to achieve quantitative, molecular level understanding of charge carriers and traps in field-doped crystalline organic semiconductors via in situ linear and nonlinear optical spectroscopy, in conjunction with transport measurements and molecular/crystal engineering. Organic semiconductors are emerging as viable materials for low-cost electronics and optoelectronics, such as organic photovoltaics (OPV), organic field effect transistors (OFETs), and organic light emitting diodes (OLEDs). Despite extensive studies spanning many decades, a clear understanding of the nature of charge carriers in organic semiconductors is still lacking. It is generally appreciated that polaron formation and charge carrier trapping are two hallmarks associated with electrical transport in organic semiconductors; the former results from the low dielectric constants and weak intermolecular electronic overlap while the latter can be attributed to the prevalence of structural disorder. These properties have lead to the common observation of low charge carrier mobilities, e.g., in the range of 10^{-5} - 10^{-3} cm^2/Vs, particularly at low carrier concentrations. However, there is also growing evidence that charge carrier mobility approaching those of inorganic semiconductors and metals can exist in some crystalline organic semiconductors, such as pentacene, tetracene and rubrene. A particularly striking example is single crystal rubrene (Figure 1), in which hole mobilities well above 10 cm^2/Vs have been observed in OFETs operating at room temperature. Temperature dependent transport and spectroscopic measurements both revealed evidence of free carriers in rubrene. Outstanding questions are: *what are the structural features and physical properties that make rubrene so unique? How do we establish fundamental design principles for the development of other organic semiconductors of high mobility?* These questions are critically important but not comprehensive, as the nature of charge carriers is known to evolve as the carrier concentration increases, due to the presence of intrinsic disorder in organic

semiconductors. Thus, a complementary question is: *how does the nature of charge transport change as a function of carrier concentration?*

To answer these questions, the PIs are extend their successful collaboration that combines transport measurements with in situ spectroscopy; the new focuses are on single crystal organic semiconductor field effect devices gated with ionic liquid or ion gel for high charge carrier doping densities. The OFET structure provides control of surface charge concentration and the determination of carrier transport characteristics (e.g. mobility), while optical spectroscopy provides physical insight into the nature of charge carriers, as polarons and free carriers possess distinct optical signatures and also provide direct measurements of the energetics of charge carriers with respect to HOMO & LUMO bands. The establishment of synergistic collaboration between transport and spectroscopy of the two laboratories over the past funding period and the successful development of a set of powerful experimental tools and model systems have now set the stage for the two PIs to tackle the most fundamental and most important problems in organic semiconductor research. A long-term outcome will be rationally designed materials and interfaces for high performance OFETs and for the exploration of new physical phenomena in organic semiconductors. In the following, we highlight most recent achievements over the past year.

4.1. Near Metallic Transport in Rubrene Electrolyte Gated Double Layer Transistors

Graduate student Wei Xie working with Frisbie employed electrolyte gating in the electric double layer transistor (EDLT) geometry to probe transport at the surface of rubrene crystals at hole densities, p, up to 6×10^{13} cm^{-2}, *i.e.*, 0.32 holes per molecule, three orders of magnitude larger than in typical OFETs, Figure X. The conductance was found to *decrease* at the highest p, a phenomenon emerging as common in organic EDLTs but incompletely understood, Figure 2b. Hall effect measurements across this conductance peak (the first of their kind) established that it is in fact a maximum in mobility at $\mu_{Hall} = 4$ cm^{2}V^{-1}s^{-1}, $p = 2.5 \times 10^{13}$ cm^{-2}, band-like transport being retained despite the large p. Cryogenic resistance-temperature (R-T) measurements down to 8 K revealed that the transport is asymmetric across this peak, being conventional at low p but suggestive of electrostatic-disorder at high p. Most significantly, around the peak conductance evidence for metallic behavior was observed including weak $R(T)$, positive dR/dT over a substantial T range, and minimum R of 50-60 kΩ, within a factor of 2 of h/e^2. Collectively, this work demonstrated transport remarkably close to a 2D metal, and

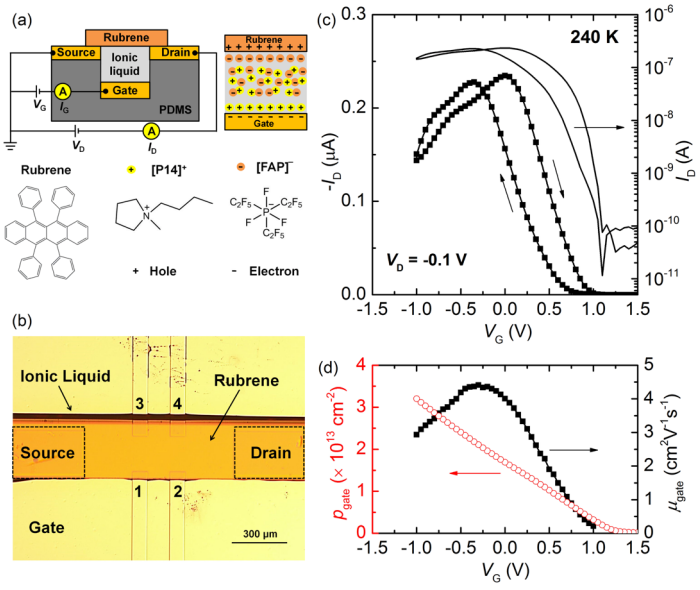

Figure 1. (a) EDLT based on rubrene. (b) Optical picture of the device. (c) I_D-V_G characteristic. (d) Mobility and charge (p) versus V_G.

suggested that with further improvements in the EDLT that true metallic transport could be obtained. The work was published in *Physical Review Letters* at the end of 2014.

4.2. Charge Saturation and Intrinsic Doping in Electrolyte-Gate Rubrene

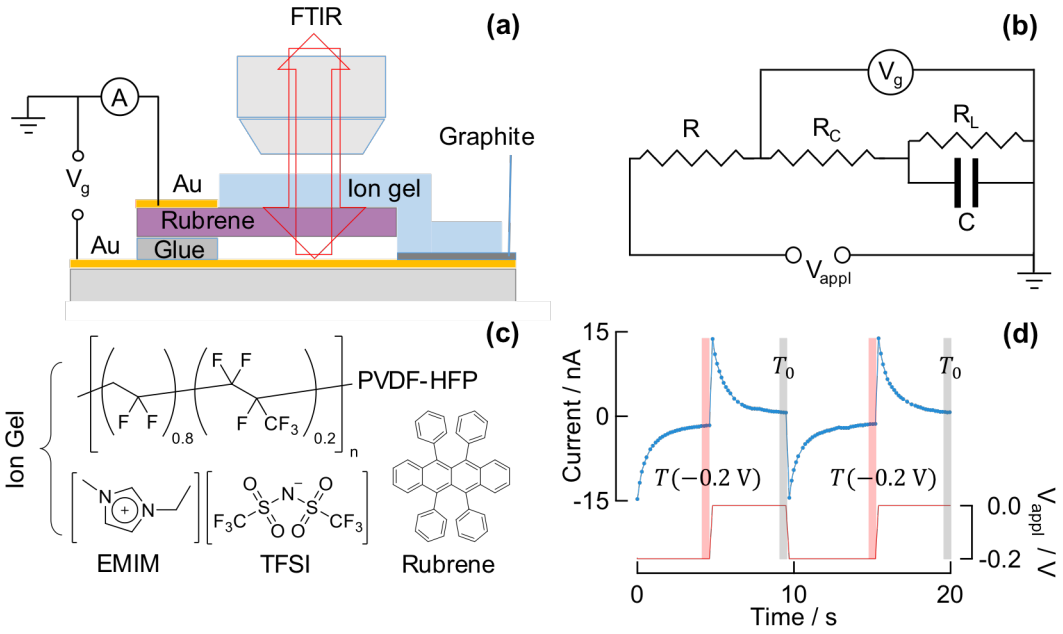

Figure 2. (a) Sample setup for the charge modulation-FTIR experiment: A $40\ nm$ Au thin film is deposited onto part of a rubrene crystal via a shadow-mask. The sample is glued and spaced from a gold electrode/mirror substrate (100 nm Au on glass). A piece of ion-gel is placed on top of the exposed rubrene (001) surface and part of the ion-gel is electrically contacted to the Au mirror with or without graphite paste. The device is connected with gold wires to a voltage source and electrometer. IR light is focused onto the device and, after reflection from the Au mirror, re-passes through the device and directed to the detector. (b) The equivalent circuit of the device. Quantitative modeling of the device gives a leakage resistance through the capacitor of $R_L = 1.0 - 0.2\ G\Omega$ (for $V_{appl} = -0.1$ to -0.8 V) and a negligible contact resistance of $R_C \sim 2\ M\Omega$ (SM1). (c) Molecular structures of the ion gel and of rubrene. The ionic liquid consists of 1-ethyl-3-methylimidazolium (EMIM) cations and bis(trifluoromethylsulfonyl)amide (TFSI) anions. The polymer matrix is poly(vinylidene fluoride-co-hexafluoropropylene) (PVDF-HFP). (d) The upper, blue graph shows the current, $\left(\frac{V_{appl}-V_g}{R}\right)$, flowing through R for two charging ($V_{appl} = -0.2$ V) and discharging ($V_{appl} = 0$ V) cycles. The lower, red graph shows the applied voltage, V_{appl}, of the corresponding cycles. The light red shade corresponds to when an CM-FTIR spectrum, $T(-0.2\ V)$, is acquired after charging, while the grey shade corresponds to when an CM-FTIR spectrum, T_0, is acquired after discharging.

Two mechanistic questions arise from the transport studies presented above: 1) does the metallic transport come from band-like carriers in single crystal rubrene? 2) what is the reason for the large carrier density even at zero gate bias? Graduate student Tim Attalah (Zhu group) and Elliot Schmidt

(Frisbie group) carried out a spectroscopic studies on the electrolyte gated rubrene single crystal. We used charge modulation infrared (CM-IR) microspectroscopy to observe the optical absorption from the electronic transitions of free charge carriers (i.e. not excitonic) in rubrene single crystal capacitors using ion gel gating dielectric, as illustrated in Fig. 2; In this experiment, a square voltage train (0-V_o volt) is applied between the rubrene single crystal and the electrolyte dielectric, while the charging-discharging current and the difference IR spectra are recorded. The change in optical density (ΔD) is obtained for each applied gate voltage (V_g), Fig. 3, referenced to V_g = 0.0 V.

For negative applied bias ($V_g < 0$ V), we see an induced absorption ($\Delta OD > 0$) over a wide spectral range, with a magnitude that increases with decreasing wavenumber. This is an optical signature qualitatively consistent with Drude absorption ($\propto 1/\omega^2$, where ω is the light frequency) of free carries. With increasingly negative bias, the IR absorption increases, in proportion to the amount of injected holes. For positive bias, we expect the rubrene to be depleted of holes and hence the IR spectrum to remain unchanged with respect to $V_g = 0$. On the contrary, we find that this bias regime exhibits bleaching, which precisely mirrors the induced-absorption features seen for $V_g < 0$ V. This bleaching shows that free-carrier like holes are already present in the rubrene at $V_g = 0$, and gradually get expelled as we increase the bias voltage.

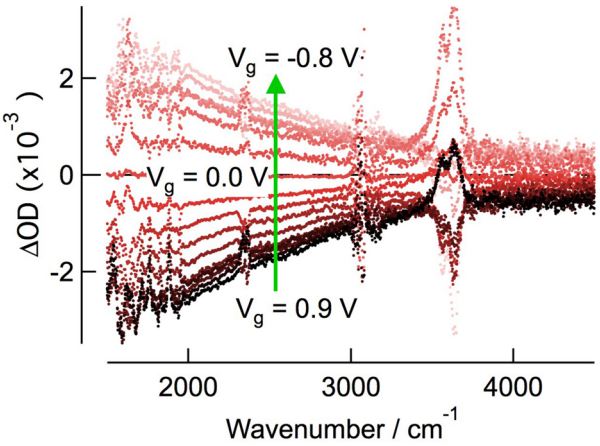

Figure 3. IR absorption spectra at difference applied voltage across the rubrene capacitor, V_g: from bottom to top, V_g = 0.9 V to V_g = -0.8 V. All spectra are referenced to that at V_g = 0 V. The broad spectral feature, which increases with decreasing wavenumber, is assigned to free-hole absorption in crystalline rubrene. The sharp peaks on top of the broad feature are vibrational peaks of the ion-gel and rubrene. The very low signal-to-noise ratio at just above $3000\ \mathrm{cm}^{-1}$ corresponds to C-H stretches in the rubrene and ion gel absorbing all of the photons of that energy range.

To trace the density of mobile holes at the rubrene surface as a function of bias voltage, we integrate ΔOD over the spectral range of the broad peak. For each spectrum (*i.e.* each value of V_g), this integral gives a scalar which is proportional to the density of optically accessible holes, $\Delta\sigma_{IR} \propto \int \Delta OD(\omega)\mathrm{d}\omega$. Since we know the total amount of charge injected into the device from the concurrent electrical measurement, we can calibrate $\Delta\sigma_{IR}$ to $\Delta\sigma_E$ in the low-bias regime (-0.2 V $< V_g < 0.2$ V) where both data sets are linear in V_g. The resulting $\Delta\sigma_{IR}$ *vs.* V_g is plotted in Fig. 4a and 4b, along with the corresponding $\Delta\sigma_E$ *vs.* V_g, for two different samples. These devices were made with different materials for the electrical contact to the IG, but nonetheless show similar results. In both samples, we see $\Delta\sigma_{IR} < 0$ for $V_g > 0$ V, that is, holes getting removed from the rubrene as the bias voltage increases from zero. The depletion only saturates for $V_g > 0.9$ V, which marks the point where (nearly) all delocalized holes have been expelled from the rubrene. This

corresponds to a density of $\sim 2\times10^{13}$ mobile holes per cm^2 present at the rubrene surface at $V_g = 0$ V.

We note that $\Delta\sigma_{IR}$ saturates also for strongly negative bias, $V_g < -0.5$ V, whereas the total

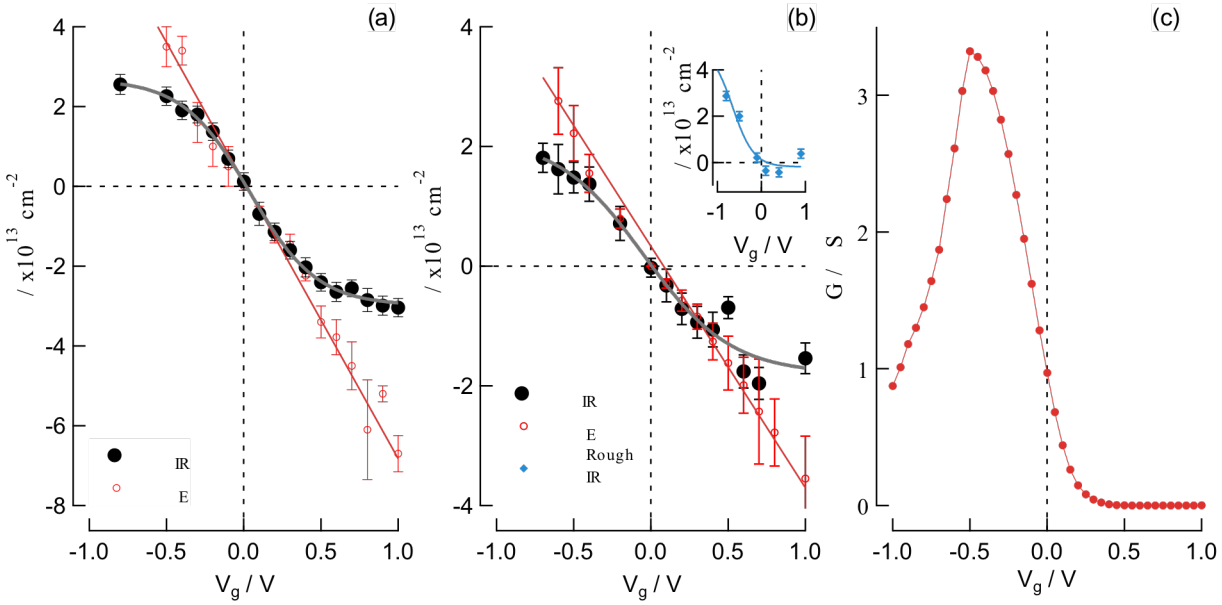

Figure 4. Surface charge density in rubrene, $\Delta\sigma$, as a function of gate bias, V_g for a device with (a) graphite and (b) gold contact to the ion gel. The solid black circles are derived from the spectroscopic signature of free-holes in rubrene, $\Delta\sigma_{IR}$, and the solid grey curves are sigmoidal fits as guides for the eye. The red dots are obtained from electrical charging/discharging measurements, $\Delta\sigma_E$ and are used to calibrate the spectroscopy data (SM 3). Error bars are the standard error of the mean determined by the averaging of charge modulation measurements. Inset in (b) shows spectroscopic $\Delta\sigma$ obtained for a device fabricated from a rough rubrene crystal and the blue curve is a sigmoidal fit as guides for the eye. (c) Conductance, G, defined as the drain current, $I_d(V_g)$, divided by the source-drain voltage, $V_{sd} = -0.1$ V, of a rubrene [EMIM][TFSI] gated transistor as fabricated in reference [13]. The device turns on when $V_g > 0$ V due to the intrinsic doping of free charge carriers seen spectroscopically. The drop in conductance when $V_g < -0.5\,V$ corresponds to the saturation of free charge carriers observed in the CM spectra.

amount of injected charge $\Delta\sigma_E$ (determined from the electrical data) remains linear in V_g over a wider range. The broad IR absorbance feature (Fig. 3) through the semiconductor selectively probes the density of mobile and delocalized carriers. Thus, the excess injection/extraction of charge beyond the saturation points in $\Delta\sigma_{IR}$ is attributed to population and depletion of more localized sites, such as deep traps or small polarons, as discussed further below.

The intrinsic (zero-bias) doping at the rubrene interface is orders of magnitude higher than any residual doping in the bare crystal, and appears upon the formation of the semiconductor/ion-gel interface. This phenomenon is also observed in transport measurement, which shows conductivity through electrolyte-gated single-crystal rubrene transistors also in the absence of applied gate voltage.[13,14] An example of such a measurement is shown in Fig. 4 (c). This kind of intrinsic doping has not been observed in rubrene devices gated with conventional dielectrics (without mobile

ions).[21–23] We conclude that there is a thermodynamic driving force for capacitive charging of the organic semiconductor/ion-gel interface. Upon forming the rubrene/ion-gel interface, the holes can latch to the surface of rubrene to stabilize the anions on the ion-gel side. This is followed by additional hole injection from the metal electrode (contacting rubrene) to reach a thermodynamic equilibrium. The opposite situation, i.e. the accumulation of electrons at the rubrene surface to stabilize cations in the electrolyte, does not occur because rubrene is predominantly a hole conductor. Holes move through rubrene with little trapping and a high mobility ($\mu_h > 1\ \mathrm{cm^2V^{-1}s^{-1}}$), while electron mobility is low ($\mu_e < 1\ \mathrm{cm^2V^{-1}s^{-1}}$) and is easily trap. As such there is a thermodynamic penalty for the electrons to de-trap and reach the interface. Furthermore, injecting electrons into rubrene from the Au electrode is also unlikely due to a large energetic offset between the rubrene conduction band and the Au Fermi level.

Further support for this intrinsic doping mechanism emerges from a comparison between devices made from optimized rubrene single crystals with smooth surfaces (Figs. 4a and 4b, main panels) and crystals with rough surfaces (Fig. 4b, inset). We obtain the latter by growing rubrene single crystals at temperatures and flow rates higher than those at optimal conditions.[27] Under these conditions, layer-by-layer growth in the rubrene *a*-*b* plane is less favorable, resulting in a rough crystalline surface topology with steps in the *c*-crystalline direction. The device with rough rubrene shows no intrinsic doping: the $\Delta\sigma_{IR}^{Rough}$ versus V_g curve shows an onset of injected hole density at $V_g = 0$ V. Since the hole mobility along the *c*-direction is much lower than that along the *a*-*b* plane and is nearly the same as electron mobility,[28] the transport of holes along the rough rubrene crystalline surface must overcome a large number of energy barriers due to steps along the *c*-direction. As a result, holes are now inhibited like electrons from reaching the rubrene/IG interface. Thus, an electric double layer cannot form without gate bias.

Having discussed the origin of the intrinsic doping, we now address the differences between $\Delta\sigma_E$ and $\Delta\sigma_{IR}$ for $|V_g| > 0.5$ V, as seen in Figs. 4a and 4b. While spectroscopic measurements reveal saturation in $\Delta\sigma_{IR}$ at both the positive and negative extremes of V_g, the electrical data indicate a linear dependence of $\Delta\sigma_E$ on V_g in the gate bias range investigated. To explain this, it is important to note that the broad IR absorbance measures mobile carriers, while the electrical measurement counts the total charge. Hence, we conclude that holes injected at $V_g < -0.5$ V occupy states that are too localized to be detected in the IR absorption. A related phenomenon is seen in measurements of electrical transport through transistor devices (Fig. 3c), where the drain-source conductance shows a decrease under moderately to strongly negative gating. Previous publications have attributed this conductance drop to trapping by anion clusters forming at larger applied biases, a model which is consistent with our data. In the positive saturation regime, $V_g > 0.5$ V, where the IR spectroscopy tells us that the rubrene is depleted of mobile holes, the linear relation between V_g and $\Delta\sigma_E$ still persists. This indicates further extraction of localized holes, *e.g.* from deep traps, which are IR-invisible and do not contribute to transport (Fig. 4c).

In summary, we carry out combined spectroscopy and electrical measurements on a model electrolyte gated organic semiconductor interface: single crystal rubrene/ion-gel. We show unambiguously the presence of a high density of intrinsic doping at the organic semiconductor/ion-gel interface. We explain this intrinsic doping as resulting from a thermodynamic driving force due to the difference in mobility of holes and electrons. Spectroscopic measurements also reveal the

saturation of free-hole like carrier density at the rubrene/ion-gel interface at $V_g < -0.5$ V, which is commensurate with the negative transconductance seen in transistor measurements.

4.3.Extending to Other Interfaces

In addition to the main research on organic semiconductor interfaces, we have also extended the research to ionic-liquid/metal and ionic-liquid/2D semiconductor interfaces. In the first set of experiments, we aimed to understand the dynamics of the double layer formation. We explored the dynamical characteristics of an IL in a metal/ionic liquid/metal (M/IL/M) capacitor. The experiments consist of frequency-dependent impedance measurements and time-dependent current vs voltage measurements for applied linear voltage ramps and abrupt voltage steps. The parameters of an equivalent circuit model are determined by fits to the impedance vs frequency data and subsequently verified by calculating the current vs voltage characteristics for the applied potential profiles. The data analysis indicates that the dynamics of the structure are characterized by a wide distribution of relaxation times spanning the range of less than microseconds to longer than seconds. Possible causes for these time scales are discussed. This work was published in *ACS Applied Materials & Interfaces.*

In the second set of experiments, we probe ionic-liquid interfaces monolayer transition-metal dichalcogenides (TMDCs) interfaces. Monolayer TMDCs show promise as model systems for two-dimensional (2D) physics and for nanoscale electronic, optoelectronic, and photonic devices. However, the prevalence of defects that serve as uncontrolled dopants, charge carrier traps, and non-radiative recombination centers stand as a major barrier to studying intrinsic 2D physics and for the realization of efficient monolayer devicesn. These effects impair electronic and optoelectronic technologies. Here we show that charged defects in MoS_2 monolayers can be effectively screened when they are in contact with an ionic liquid (IL), leading to an increase in photoluminescence (PL) yield by up to two-orders of magnitude. The extent of this PL enhancement by the IL correlates with the brightness of each sample. We propose the existence of two classes of non-radiative recombination centers in monolayer MoS_2: (i) charged defects that relate to unintentional doping and may be electrostatically screened by ILs and (ii) neutral defects that remain unaffected by the presence of ILs. This work is under review at *J. Phys. Chem. Lett.*

5. Publications Acknowledging DOE support

Wang, S; Ha, MJ; Manno, M; Frisbie, CD; Leighton, C. "Hopping transport and the Hall effect near the insulator-metal transition in electrochemically gated poly(3-hexylthiophene) transistors." *Nature Communications,* **2012***, 3,* 1210. DOI: 10.1038/ncomms2213

Morris, J. D.; Atallah, T. L.; Park, H.; Ooi, Z.; Dodabalapurd, A.; Zhu, X.-Y. "Quantifying space charge accumulation in organic bulk heterojunctions by nonlinear optical microscopy," *Organic Electronics* **2013**, *14*, 3014-3018.

Morris, J. D.; Atallah, T. L.; Lombardo, C. J.; Dodabalapur, A.; Zhu, X.-Y. "Mapping electric field distributions in biased organic bulk heterojunctions under illumination by nonlinear optical microscopy," *Appl. Phys. Lett.* **2013**, *102*, 033301.

Xie, W.; Wang, S.; Zhang, X.; Leighton, C.; Frisbie, C. D. "High Conductance 2D Transport around the Hall Mobility Peak in Electrolyte-Gated Rubrene Crystals", *Phys. Rev. Lett*., **2014**, *113*, 246602.

Atallah, T.; Gustafson, M. Schmidt, Elliot; Frisbie, C. Daniel; Zhu, X.-Y. "Charge Saturation and Intrinsic Doping in Electrolyte-Gated Organic Semiconductors," *J. Phys. Chem. Lett.* **2015**, *6*, 4840-4844

Schmidt, Elliot, Sha Shi, P. Paul Ruden, and C. Daniel Frisbie, "Characterization of the Electric Double Layer Formation Dynamics of a Metal/Ionic Liquid/Metal Structure," *ACS Applied Materials & Interfaces* **2016**, *8*, 14879-14884.

T. L. Atallah, J. Wang, M. Bosch, D. Seo, R. A. Burke, O. Moneer, Justin Zhu, M. Theibault, L. E. Brus, J. Hone, X.-Y. Zhu, "Electrostatic Screening of Charged Defects in Monolayer MoS_2," *J. Phys. Chem. Lett.* **2017,** under review.

6. People worked on the project

Tim Atallah (graduate student, 100%), Elliot Schmidt (graduate student, 100%).

7. Estimate of the unexpended funds at the end of project period.

$0.00